Title: Toward Tungsten Electrodeposition at Moderate Temperatures Below 100 °C Using Chloroaluminate Ionic Liquids

Author Names:

Shota Higashino,[1,2,*] Yoshikazu Takeuchi,[2] Masao Miyake,[2] Takuma Sakai[1], Takumi Ikenoue,[2] Masakazu Tane,[1] and Tetsuji Hirato[2]

Affiliations:

[1]Graduate School of Engineering, Osaka Metropolitan University, Sugimoto, Sumiyoshi-ku, Osaka 558-8585, Japan

[2]Graduate School of Energy Science, Kyoto University, Yoshida-honmachi, Sakyo-ku, Kyoto 606-8501, Japan

*Corresponding Author: higashino@omu.ac.jp

Abstract

The electrodeposition of tungsten at moderate temperatures (<100 °C) has been of significant interest for the fabrication of thin films and microelectromechanical system components to decrease energy consumption and increase process safety. In this study, we investigated the electrochemical reduction of WCl_4 and WCl_5 in 1-ethyl-3-methylimidazolium chloride (EMIC) and EMIC–$AlCl_3$ ionic liquids at 80–120 °C. W-rich films with a thickness of approximately 1 μm were obtained from the Lewis acidic EMIC–$AlCl_3$–WCl_5 bath, whereas the other baths did not yield any deposits. The films obtained from the EMIC–$AlCl_3$–WCl_5 bath at 80 °C had higher W contents of 54 at.% than those obtained at 120 °C. X-ray absorption near-edge structure spectra of the W-rich films indicated that W existed in an oxidized state. The findings of this study can be used as a guide to explore optimal electrolytes and electrolytic conditions for the electrodeposition of metallic W at moderate temperatures.

Introduction

Tungsten is widely used as a heat-resistant material owing to its high melting point, low thermal expansion ratio, and high chemical stability. Consequently, the electrodeposition of W has attracted significant interest in the fabrication of thin films[1] and microelectromechanical system components using the lithographie (lithography), galvanoformung (electroplating), and abformung (molding) (LIGA) process.[2,3]

However, although the redox potential of W is not significantly negative compared to the reduction potential of water to hydrogen,[4] the electrodeposition of W from aqueous solutions has never been achieved. Therefore, several researchers have investigated the electrodeposition of W using high-temperature molten salts, including fluorides,[5] bromides,[6] chlorides,[7] and their mixtures,[1,8–12] and successfully obtained thick and dense W films. However, such systems generally require high temperatures (>250 °C), rendering the process highly energy-consuming. In addition, during the LIGA process, high temperatures result in thermal expansion and, consequently, the deterioration of the mold and substrate, which significantly hinders the process.[13] Therefore, the electrodeposition of W at moderate temperatures (<100 °C) is worth exploring.

Several reports on the electroreduction of W at moderate temperatures are available in the literature. Scheffler et al. reported that WCl_6 and $KWCl_6$ can be reduced in basic 1-ethyl-3-methylimidazolium chloride (EMIC)–$AlCl_3$ ionic liquids (ILs).[14] Cavinato et al. obtained W-rich deposits using a Lewis acidic $AlCl_3$–NaCl bath containing WCl_6 and revealed that the W in the deposits had an oxidation state between 0 and +2.[15] Although the bath temperature is not specified mentioned in their report, it is assumed to be higher than 107 °C, which is the eutectic point of the Lewis acidic $AlCl_3$–NaCl system.[16] W-rich deposits have also been obtained from Lewis acidic EMIC–$AlCl_3$ ILs containing $K_3W_2Cl_9$ and W_6Cl_{12};[17,18] based on X-ray photoelectron spectroscopy results, these deposits are in an oxidized state.

However, to the best of our knowledge, no comparative studies have been conducted on the electroreduction of W at moderate temperatures in baths with different compositions. Furthermore, the relationship between electrolytic conditions and the deposition behavior of W films remains unclear. In this study, we conducted a comparative analysis of the

electroreduction of W species at moderate temperatures (80 and 120 °C) in EMIC and EMIC–$AlCl_3$ ILs containing WCl_4 or WCl_5. The electrochemical behavior of W in different baths was investigated to determine the optimal bath for obtaining W-containing films. In addition, the morphologies, structures, compositions, and chemical states of the obtained films were investigated.

Experimental

Purification of reagents and preparation of electrolytic baths

EMIC (97%, Tokyo Chemical Industry) was dried under vacuum at 120 °C before use; the water content of the EMIC after drying was less than 10 ppm, as measured via Karl Fischer coulometric titration (MKC610, Kyoto Electronics Manufacturing). $AlCl_3$ (99%, Wako) was purified through sublimation from an $AlCl_3$–NaCl molten salt mixed with Al wires (99.999%, Nilaco).[19] EMIC–$AlCl_3$ baths were prepared by mixing EMIC and $AlCl_3$ at a molar ratio of 1:1.5 in an Ar-filled glove box (DBO-1KH-HMK, Miwa MFG) with a dew point below −70 °C.

WCl_4 (>95%, Sigma Aldrich) and WCl_5 (>99%, Kojundo Chemical Laboratory) were heated in vacuum-sealed Pilex glass tubes to remove tungsten oxychloride contaminants.[14] The glass tubes were placed in a horizontal furnace such that WCl_4 and WCl_5 were heated at a fixed temperature, and the other ends of the tubes were exposed to ambient temperature. WCl_4 and WCl_5 were heated to 325 and 100 °C, respectively, for 24 h. During heating, orange tungsten oxychloride crystals precipitated at the cool ends of the Pilex tubes. Potassium fluoride (>99.9%, Sigma Aldrich) was used as received. WCl_4, WCl_5, and KF were added to the EMIC–$AlCl_3$ baths in an Ar-filled glove box to prepare electrolytic baths.

Electrochemical measurements

Electrochemical measurements were performed in an Ar-filled glove box (DBO-1KH-HMK, Miwa MFG) with a dew point below −70 °C using electrochemical analyzers (ALS model 660C and Hokuto Denko HZ 7000). A 25 mL glass vessel served as the electrolytic cell. The bath temperature was maintained at 80 or 120 °C using an Al block and a hot magnetic

stirrer. Cyclic voltammograms were recorded using a Pt electrode as the working electrode and an Al plate (99.99%, Nilaco) as the counter electrode. The reference electrode was an Al wire (99.999%, Nilaco) immersed in an EMIC–$AlCl_3$ (molar ratio of 1:2) IL, prepared in a similar manner to previous studies.[20,21] A porous glass frit was used as a separator between the bath and reference electrode. Potentiostatic electrodeposition was performed on a Cu rod electrode with a diameter of 5.5 mm (99.994%, Nilaco) to facilitate subsequent characterizations. The side of the Cu rod electrode was covered with a fluororesin heat-shrinking tube (FEP-060; Junkosha). An Al coil made of Al wire (99.999%, Nilaco) and an Al reference electrode were used as the counter and reference electrodes, respectively. The bath was agitated at 150 rpm using a magnetic stirrer bar (8.0 mm × Φ1.5 mm).

Characterization of deposits

The morphologies of the Cu electrode after electrodeposition were observed using scanning electron microscopy (SEM; JSM-6510LV, JEOL). The elemental compositions of the deposits were analyzed using an energy-dispersive X-ray (EDX) spectrometer (INCAx-act, Oxford Instruments) mounted on an SEM system. X-ray diffraction (XRD) patterns were obtained using an X-ray diffractometer (X'pert PRO-MPD, PANalytical) with Cu-*Kα* radiation.

X-ray absorption near edge structure (XANES) spectra of the deposits were recorded at the beamline BL11 of the Kyushu Synchrotron Light Research Center (SAGA-LS, Japan) equipped with a Si(111) double-crystal monochromator and ionization chamber detectors. The W L_3-edge XANES spectra of the deposits were obtained in transmission mode. Metallic W (1 μm powder, 99.95%, Nilaco) and tungsten(IV) oxide powder (99.9%, Kojundo Chemical Laboratory) were used as reference samples; the reference samples were mixed with boron nitride powder (99%, Kojundo Chemical Laboratory) and pressed to form pellets. The deposits were obtained on Cu films (10 μm-thick, 99.9%, Nilaco) and sealed in a polyethylene bag in an Ar-filled glove box. The XANES data were analyzed using the Athena program in the Demeter 0.9.26 software.[22] XANES measurements were performed at room temperature (25 °C).

Results and discussion

Bath composition

The bath compositions used in this study are listed in Table 1. Both WCl_4 and WCl_5 were highly soluble in neat EMIC and relatively less soluble in the Lewis acidic EMIC–$AlCl_3$ IL, indicating the Lewis acidic characteristics of WCl_4 and WCl_5. The EMIC–WCl_4 and EMIC–WCl_5 mixtures formed a homogeneous liquid at temperatures ≥80 °C when the ratio of EMIC:WCl_X (X = 4 or 5) was 1:0.1 and were therefore chosen as the bath composition. EMIC–$AlCl_3$–WCl_4 and EMIC–$AlCl_3$–WCl_5 baths were prepared by saturating WCl_4 and WCl_5, respectively, in the EMIC–$AlCl_3$ ILs.

Table 1. Bath compositions used in this study. Molar concentrations of W species were calculated using the density values of pure EMIC and EMIC–1.5$AlCl_3$ ILs at 80 °C reported in the literature.[23]

Bath	Composition (molar ratio)	Concentration of W species (mM)
EMIC–WCl_4	1:0.1	800
EMIC–WCl_5	1:0.1	800
EMIC–$AlCl_3$–WCl_4	1:1.5:1.2 × 10^{-4} (saturated)	0.5
EMIC–$AlCl_3$–WCl_5	1:1.5:3.0 × 10^{-2} (saturated)	100

Cyclic voltammetry (CV)

Figure 1 shows the cyclic voltammograms of Pt electrodes in the baths listed in Table 1. CV curves of the neat EMIC and EMIC–$AlCl_3$ baths were also compared. The potential sweep started from the open circuit potential (OCP) of the Pt electrode, referred to as the Al quasi-reference electrode. The CV curve of the neat EMIC bath (Fig. 1a) exhibited an electrochemical window of approximately 2 V, which was determined via cathodic EMI^+ decomposition (−1.7 V) and anodic Cl_2 generation (+0.3 V). The CV curves of the EMIC–WCl_4 and EMIC–WCl_5 baths (Fig. 1b and c, respectively) show four cathodic waves (C1–C4) and two anodic waves

(A1 and A2) within the electrochemical window of EMIC. Two evident redox couples C1/A2 and C3/A1 were also observed in a Lewis basic EMIC–$AlCl_3$ containing W^{5+} species, and they could be attributed to redox of W^{5+}/W^{4+} and W^{4+}/W^{3+}, respectively.[14] C4 could be reduction of W^{3+} species to a lower valence state. Although the cathodic reaction for C2 remains unclear, it might be reduction of impurities in the bath such as protonic species.[14] We conducted potentiostatic electrolysis on a Cu electrode at −1.5 V in these two baths; however, no deposits were obtained. Therefore, we consider that only soluble species were generated by the electroreduction of W species in these two baths.

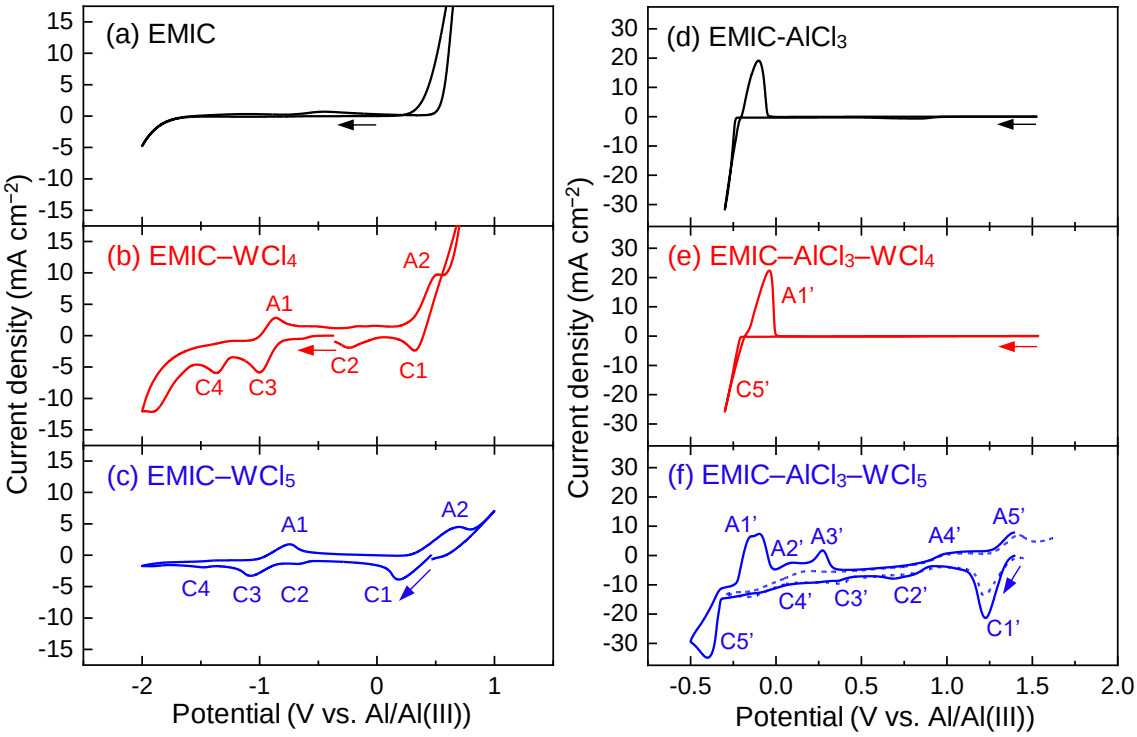

Figure 1. Cyclic voltammograms on a Pt electrode in (a) neat EMIC, (b) EMIC–WCl_4, (c) EMIC–WCl_5, (d) EMIC–$AlCl_3$, (e) EMIC–$AlCl_3$–WCl_4, and (e) EMIC–$AlCl_3$–WCl_5 baths at 120 °C. The dotted line in (f) shows a CV curve where the potential scan was reversed at a more positive potential (−0.3 V). The potential scan rate was 10 mV s^{-1}. The arrow in each graph indicates the OCP at which the potential scan was started.

The CV of the EMIC–$AlCl_3$ bath in Fig. 1d shows a pair of cathodic and anodic waves at approximately −0.3 V, which are attributed to the deposition and stripping of Al, respectively. The CV profile of the EMIC–$AlCl_3$–WCl_4 bath was almost identical to that of the EMIC–$AlCl_3$ bath and did not exhibit any reduction current for WCl_4, indicating that WCl_4 was electrochemically stable in the EMIC–$AlCl_3$–WCl_4 bath. Notably, in the EMIC–$AlCl_3$–WCl_4, EMIC–WCl_4, and EMIC–WCl_5 baths, the potentiostatic electrolysis on a Cu electrode at approximately +0.1 V did not yield any deposit.

The CV of the EMIC–$AlCl_3$–WCl_5 bath (Fig. 1f) shows at least four cathodic and anodic current waves (C1′–C4′ and A2′–A5′, respectively) between the OCP and Al deposition/stripping potential at approximately −0.3 V, noted as C5′ and A1′, respectively. C1′–C4′ are attributed to the reduction of WCl_5. The anodic waves A1′ and A2′ were not observed when the potential scan was reversed at −0.3 V, as shown by the dotted line in Fig. 1(f), indicating that these two anodic waves correspond to the anodic dissolution of the Al and Al–W formed during the cathodic scan toward more negative potentials than −0.3 V.[17] A3′–A5′ were attributed to the oxidation of W species generated by the reduction WCl_5 (C3′ and C4′). C1′/A5′ appear to be the redox couple of W^{5+}/W^{4+}. C1′/A5′ in the EMIC–$AlCl_3$–WCl_5 bath, as well as C1/A2 and C3/A1 in the EMIC–WCl_4 and EMIC–WCl_5 baths, could be possible through exchanging Cl^- between W and Al species.[24] C2′–4′ could be reduction of W^{4+} species to a further lower valence state. Notably, potentiostatic electrolysis on Cu electrodes in the EMIC–$AlCl_3$–WCl_5 bath yielded W-containing deposits. The characterization of these deposits is described below.

Potentiostatic electrolysis

Potentiostatic electrolysis on Cu electrodes was performed in the EMIC–$AlCl_3$–WCl_5 bath at 80 and 120 °C. The potentials applied were +0.1 and +0.4 V, which are close to the C4′ and C3′ waves shown in Fig. 1(f), respectively. At these potentials, the reduction of Al species (C5′ in Fig. 1(f)) does not occur, and thus, only the reduction of W species could be investigated. The charge density was set such that it yielded a metallic W film with a thickness of approximately 2 μm. The typical cathodic current-time transients and average current density

during electrolysis are shown in Fig. 2. The current-time transients (Fig. 2(a)) showed an initial spike, followed by a decrease to a steady state. These current transients were attributed to the initial nucleation and subsequent diffusion-limited growth.[25] The average current density (Fig. 2(b)) increased with increasing temperature and negative potential. Furthermore, the current density values observed in the EMIC–$AlCl_3$–WCl_5 bath were significantly higher than those observed in the EMIC–$AlCl_3$–W_6Cl_{12} bath (0.3 and 0.1 mA cm^{-2} at +0.1 and +0.4 V, respectively, at 80 °C) in our previous study,[18] owing to the higher molar concentration of WCl_5 than that of W_6Cl_{12} (49 mM).

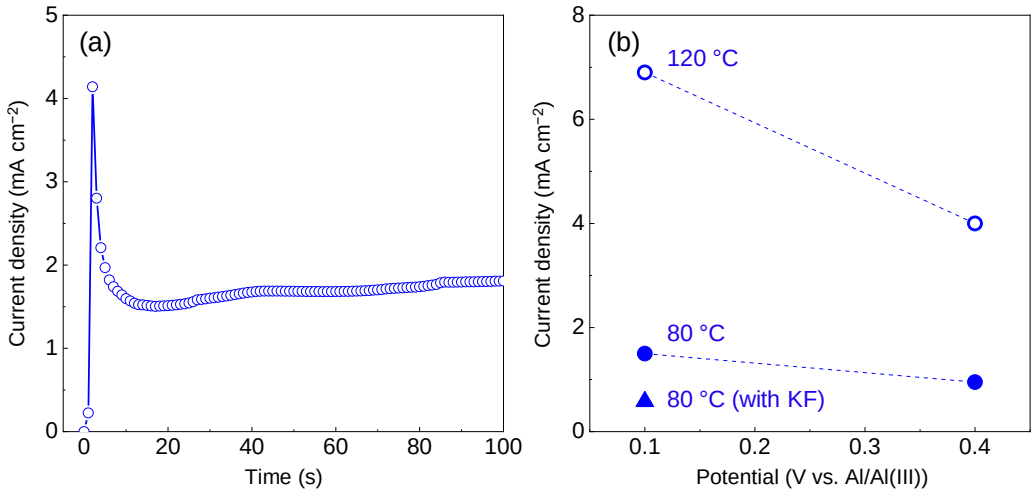

Figure 2. (a) Cathodic current-time transients during potentiostatic electrolysis in the EMIC–$AlCl_3$–WCl_5 bath at +0.1 V and 80 °C. (b) Average cathodic current density during potentiostatic electrolysis in EMIC–$AlCl_3$–WCl_5 baths at +0.1 and +0.4 V and 80 and 120 °C. In (b), current density during potentiostatic electrolysis in the EMIC–$AlCl_3$–WCl_5–KF bath at +0.1 V and 80 °C is denoted as "80 °C (with KF)."

As shown in Fig. 3, black deposits are obtained on the Cu electrodes after electrolysis. The deposits were prone to exfoliation from the Cu electrode during the washing process after electrolysis. The deposits obtained after electrolysis at +0.4 V at 80 and 120 °C were dispersed

and did not show a film-like morphology. In particular, at +0.4 V and 120 °C, the deposits could not be clearly observed owing to the etched surface of the Cu electrode. The deposits obtained at +0.1 V were composed of granular grains and exhibited a film-like morphology. The compactness of the films obtained at +0.1 V and 80 °C was evidenced by the cross-sectional SEM image shown in the inset in Fig. 3. The thickness of the compact part of the film was estimated to be approximately 1 μm. Considering the charge density, the current efficiency was estimated to be 40%.

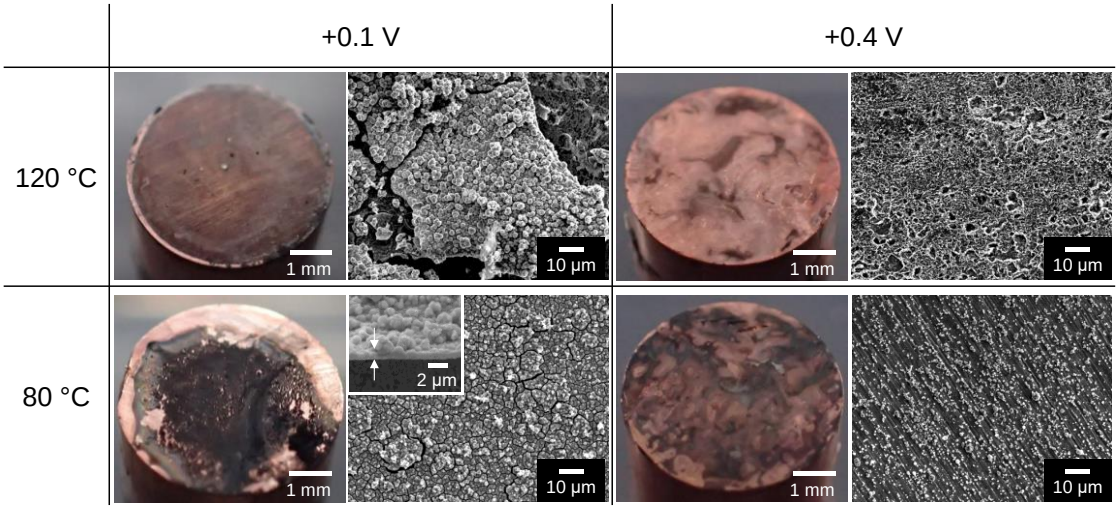

Figure 3. Typical photographs and SEM images of the Cu substrate surfaces after potentiostatic electrolysis in EMIC–$AlCl_3$–WCl_5 baths at +0.1 and +0.4 V and 80 and 120 °C. The inset in the SEM image for +0.1 V at 80 °C shows a typical cross-sectional SEM image of the deposit.

Elemental compositions of the deposits

EDX spectra of the deposits were obtained to analyze their elemental compositions (Fig. 4). The EDX spectra exhibit intense peaks for C, O, Cu, W, Al, and Cl. Cu was derived from the electrode, and its amount changed depending on the amount of the deposit that remained on the Cu substrate after washing. Al, C, and certain amounts of O and Cl were derived from the bath components that were attached to the W deposits.

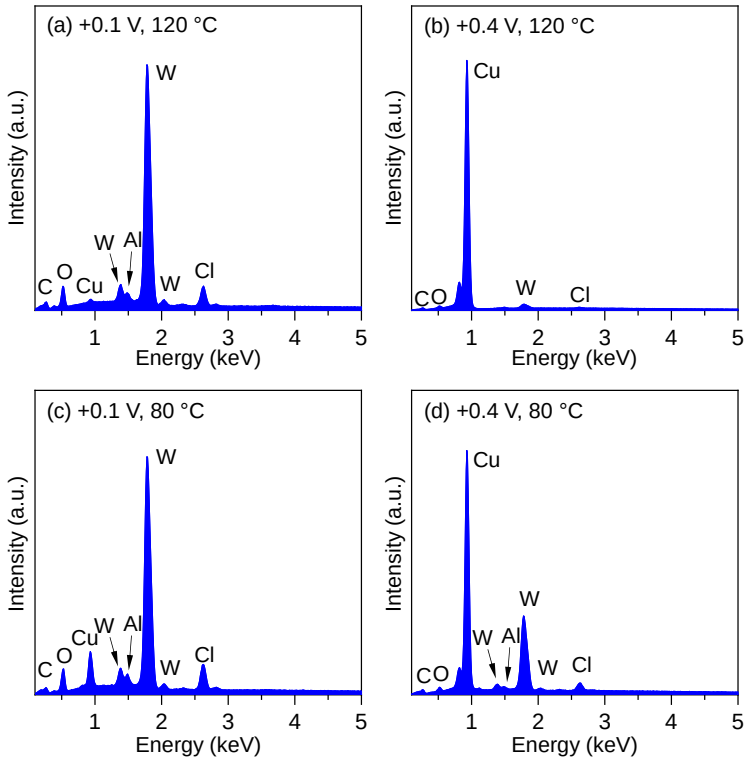

Figure 4. EDX spectra of Cu substrate surfaces after potentiostatic electrolysis in the EMIC–$AlCl_3$–WCl_5 bath at +0.1 and +0.4 V and 80 and 120 °C.

As shown in the elemental composition chart in Fig. 5, the deposits obtained at 80 °C exhibit a higher W content than those obtained at 120 °C at both +0.1 and +0.4 V. Furthermore, the W contents of the deposits obtained at +0.1 and +0.4 V at 80 °C were higher than those obtained in our previous study for deposits formed from Lewis acidic EMIC–$AlCl_3$–W_6Cl_{12} baths at more positive potentials than +0.1 V.[18]

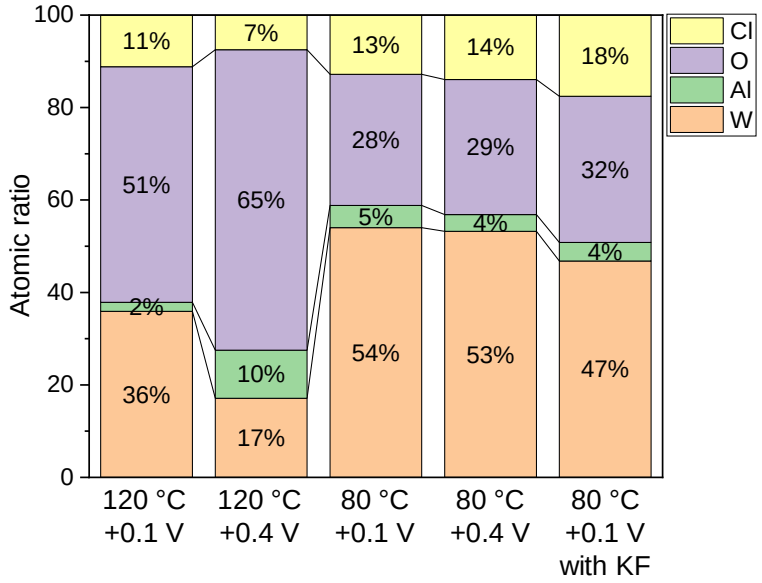

Figure 5. Elemental compositions of the deposits obtained via potentiostatic electrolysis in the EMIC–$AlCl_3$–WCl_5 bath at +0.1 and +0.4 V and 80 and 120 °C. Composition of the deposit obtained from the KF-added bath at +0.1 V and 80 °C is presented as "80 °C +0.1 V with KF."

The presence of Cl in the deposits may indicate that the deposits are not metallic W, but W–Cl species, as indicated in the literature.[15] XANES spectra were therefore obtained to investigate this hypothesis. Meanwhile, as the EMIC–$AlCl_3$–WCl_5 bath did not have an O source, the presence of O in the deposits was presumed to originate from the oxide or hydroxide layers that formed on the deposit surfaces during the sample transfer from the glove box to the SEM/EDX analysis chamber. The EDX spectrum of the region of the Cu substrate where the deposits were completely exfoliated (Supplementary Figure S1) showed only small amounts of O and Si, which could be attributed to surface oxide or hydroxide and SiC particles that remained after polishing, respectively, indicating that the O detected on the deposits was derived from the surface oxidation and hydration of the deposits. The deposits obtained at 80 °C exhibited a lower O content (and higher W content) than those obtained at 120 °C, probably because the former had smoother morphologies, as shown in Fig. 3. The films exhibiting rougher and cracked morphologies would enhance surface oxidation. The rougher the surface of the deposit is, the more oxygen atoms diffuse into the deposit and the faster the oxidation proceeds. [26]

Effects of KF addition

In previous reports on W electrodeposition from molten salts, KF was added to the bath to obtain deposits with fine grains and smooth morphologies.[2] The effects of KF on W electroreduction were also examined in this study, with the expectation that the smooth morphologies of the deposits would reduce the O content derived from the surface oxidation layer.

KF was added to the EMIC–$AlCl_3$–WCl_5 bath at a molar ratio of EMIC:$AlCl_3$:WCl_5:KF = 1:1.5:3.0 × 10^{-2}:0.1. The current density value observed during electrolysis in the EMIC–$AlCl_3$–WCl_5–KF bath is of the same order as that of the current density of the bath without KF at +0.1 V and 80 °C, as shown in Fig. 2. Furthermore, the deposit obtained in the EMIC–$AlCl_3$–WCl_5–KF bath at +0.1 V and 80 °C has a relatively smooth surface (Fig. 6a) compared to that obtained without KF (lower-left SEM image in Fig. 3). However, cracks inevitably form even with KF addition, and the EDX spectrum (Fig. 6b) and the calculated elemental composition (the rightmost column in Fig. 5) show the presence of both O and Cl at similar molar ratios to those observed in the deposits obtained without KF (the middle column in Fig. 5).

We also performed potentiostatic electrolysis using a Ni electrode in the EMIC–$AlCl_3$–WCl_5–KF bath at +0.1 V and 80 °C, which yielded a deposit with similar morphology and composition to that obtained using a Cu electrode (Supplementary Figure S2). This implies that the electrode material does not significantly affect the quality of the deposit.

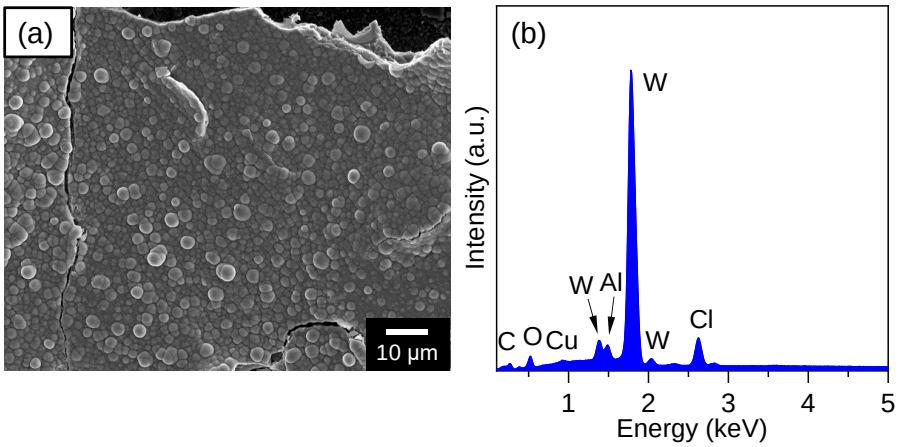

Figure 6. SEM image and EDX spectrum of Cu electrode surfaces after potentiostatic electrolysis in the EMIC–$AlCl_3$–WCl_5–KF bath at +0.1 V and 80 °C.

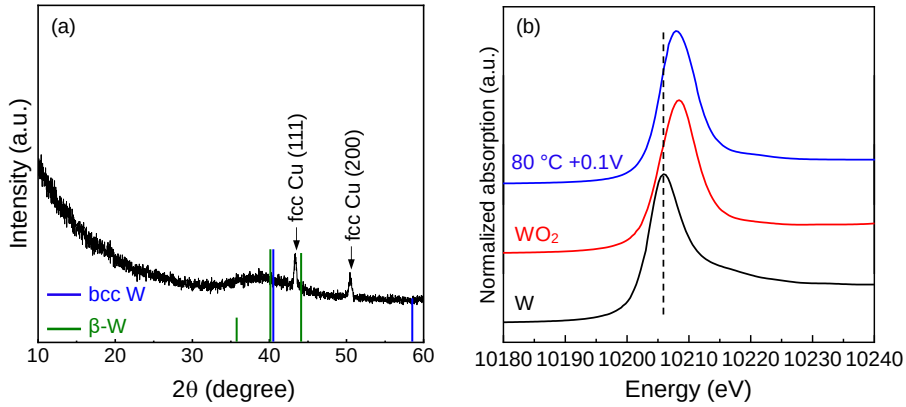

Figure 7. (a) XRD pattern and (b) XANES spectra of the deposit obtained after potentiostatic electrolysis in the EMIC–$AlCl_3$–WCl_5 bath at +0.1 V and 80 °C. Reference peak positions for bcc W (ICDD PDF No. 00-004-0806) and β-W (ICDD PDF No. 00-047-1319) are presented for comparison in (a). XANES spectra for pure W metal and WO_2 are presented for comparison in (b).

Crystallographic phase and oxidation state of the deposit

The W-rich deposit obtained at +0.1 V and 80 °C, which had the highest W content among the as-obtained deposits (Fig. 5), was further characterized using XRD and XANES. The XRD pattern (Fig. 7a) did not show any peak corresponding to bcc W or β-W,[6] only showing a halo

peak at approximately $2\theta = 39°$, which indicated that the deposit was amorphous. The XRD pattern also exhibited fcc Cu peaks derived from the Cu substrate.

The W L_3-edge XANES spectrum of the deposit was compared to the spectra of metallic W and WO_2 (Fig. 7b). Note that the XANES spectra were recorded in transmission mode, and therefore indicated the oxidation state of W inside the films rather than near the surface. The XANES spectrum of the W L_3-edge was characterized by an absorption at approximately 10207 eV, which shifted toward a higher energy value when the oxidation state of W increased from 0 to +4, corresponding to metallic W and WO_2, respectively. The XANES spectrum of the deposit was located closer to that of WO_2 than that of metallic W. This indicates that the W in the deposit was in an oxidized state rather than a metallic state. From EDX and XANES analysis, it was inferred that the deposit was originally composed of W and Cl and that the Cl was replaced by O when the deposit was exposed to air when transported for characterization.

As in the case of the EMIC–$AlCl_3$–WCl_5 bath, the electrochemical reduction of W species in the EMIC–WCl_5 and EMIC–WCl_4 baths might have yielded W-rich substances containing Cl, but they dissolved in the baths. As presented in Table 1 and in previous reports,[17,27,28] W–Cl species with a low oxidation state of ≤4 have low solubility in Lewis acidic EMIC–$AlCl_3$ baths. Therefore, solid deposits were obtained in Lewis acidic baths.

However, the reason that the EMIC–$AlCl_3$–WCl_4 bath yielded no deposits is still unclear. In this bath, WCl_4 seemed to be electrochemically stable, as shown in the CV curve (Fig. 1(e)). It is possible that WCl_4 has different dissolved structures in an acidic bath than in a basic bath, which led to their different electrochemical behavior. Spectroscopic techniques such as UV-Visible,[29] Raman,[30] and EXAFS[28,31] will be used to obtain information about the dissolved structures of WCl_4 in future studies.

The electrodeposition of W-rich films at temperatures below 100 °C, which was achieved in the present study, can be applied to thin-film forming processes for W-based materials by combining the electrodeposition of W-rich films with a subsequent annealing process in a suitable atmosphere to transform W-rich films to desired materials. For example, the formation of WC by combining the chemical vapor deposition of WO_3 with a subsequent heat treatment has been demonstrated in a previous study.[32]

It is worth exploring optimal electrolytes, electrolytic conditions, and more effective additives than KF to obtain W-rich films with lower Cl and O contents or metallic W films at moderate temperatures. We believe that the findings of this study can also be applied to electrodeposition of other refractory metals such as Mo at moderate temperatures.[33]

Conclusions

In this study, the electroreduction of W species in EMIC and EMIC–$AlCl_3$ baths with WCl_4 or WCl_5 at 80 and 120 °C was compared. Approximately 1 μm-thick W-rich films were obtained in the EMIC–$AlCl_3$–WCl_5 bath at +0.1 V at temperatures below 100 °C. In contrast, the EMIC–$AlCl_3$–WCl_4, EMIC–WCl_4, and EMIC–WCl_5 baths did not yield any solid deposits. The W-rich film obtained from the EMIC–$AlCl_3$–WCl_5 bath contained a high W content, exceeding 50%. Adding KF to the EMIC–$AlCl_3$–WCl_5 bath smoothened the film morphology but did not significantly affect the film composition. XRD and XANES analyses indicated that the W-rich films were amorphous and contained W in an oxidized state. The findings of this study can be used for guiding the electrodeposition of W at temperatures below 100 °C, which can significantly reduce energy consumption and increase safety during industrial applications.

Acknowledgements

XANES experiments were performed at beamline BL11 of the SAGA-LS (Proposal No. 2207068F). We thank Dr. Hiroyuki Setoyama for his support on XANES measurements. This study was financially supported by Japan Society for the Promotion of Science (JSPS) Research Fellowship for Young Scientists (DC2, No. 19J14672), JSPS Overseas Challenge Program for Young Researchers (No. 201980512), and JSPS KAKENHI Grant-in-Aid for Research Activity Start-up (No. 21K20493). We would like to thank Editage (www.editage.com) for English language editing.

Declaration of Competing Interest

The authors declare no competing interests.

References

1. X. Meng, Y. Norikawa, and T. Nohira, *Electrochem. Commun.*, **132**, 107139 (2021).

2. H. Nakajima et al., *Electrochim. Acta*, **53**, 24–27 (2007).

3. K. Nitta et al., *Electrochim. Acta*, **53**, 20–23 (2007).

4. M. Pourbaix, *Atlas of Electrochemical Equilibria in Aqueous Solutions*, National Association of Corrosion Engineers, (1974).

5. S. Senderoff and G. W. Mellors, *J. Electrochem. Soc.*, **114**, 586 (1967).

6. A. Katagiri, M. Suzuki, and Z. Takehara, *J. Electrochem. Soc.*, **138**, 767–773 (1991).

7. M. Masuda, H. Takenishi, and A. Katagiri, *J. Electrochem. Soc.*, **148**, C59 (2001).

8. T. Nohira, T. Ide, X. Meng, Y. Norikawa, and K. Yasuda, *J. Electrochem. Soc.*, **168**, 046505 (2021).

9. H. Nakajima, T. Nohira, and R. Hagiwara, *Electrochem. Solid-State Lett.*, **8**, C91 (2005).

10. V. V. Malyshev, *Prot. Met. Phys. Chem. Surf.*, **45**, 373–390 (2009).

11. O. Takeda, S. Watanabe, C. Iseki, X. Lu, and H. Zhu, *J. Electrochem. Soc.*, **169**, 122503 (2022).

12. Y. Norikawa, X. Meng, K. Yasuda, and T. Nohira, *J. Electrochem. Soc.*, **169**, 102506 (2022).

13. K. Nitta, T. Nohira, R. Hagiwara, M. Majima, and S. Inazawa, *Electrochim. Acta*, **55**, 1278–1281 (2010).

14. T. B. Scheffler and C. L. Hussey, *Inorg. Chem.*, **23**, 1926–1932 (1984) http://dx.doi.org/10.1021/ic00181a027.

15. A. G. Cavinato, G. Mamantov, and X. B. Cox, *J. Electrochem. Soc.*, **132**, 1136–1140 (1985).

16. E. M. Levin, J. F. Kinney, R. D. Wells, and J. T. Benedict, *J. Res. Natl. Bur. Stand., A. Phys. Chem.*, **78A**, 505–507 (1974).

17. T. Tsuda et al., *J. Electrochem. Soc.*, **161**, D405–D412 (2014).

18. S. Higashino, M. Miyake, H. Fujii, A. Takahashi, and T. Hirato, *J. Electrochem. Soc.*, **164**, D120–D125 (2017).

19. R. C. Howie and D. W. Macmillan, *Inorg. Nucl. Chem. Letters*, **6**, 399–401 (1970).

20. T. Tsuda et al., *J. Electrochem. Soc.*, **161**, D405–D412 (2014).

21. T. Tsuda, C. L. Hussey, and G. R. Stafford, *J. Electrochem. Soc.*, **151**, C379–C384 (2004).

22. B. Ravel and M. Newville, *J. Synchrotron Radiat.*, **12**, 537–541 (2005).

23. A. A. Fannin et al., *Journal of Physical Chemistry*, **88**, 2614–2621 (1984).

24. P. Giridhar, B. Weidenfeller, S. Z. El Abedin, and F. Endres, *Phys. Chem. Chem. Phys.*, **16**, 9317–9326 (2014).

25. A. Radisic, F. M. Ross, and P. C. Searson, *J. Phys. Chem. B*, **110**, 7862–7868 (2006).

26. L. Wang et al., *Acta Metall. Sin. (Engl. Lett.)*, **28**, 381–385 (2015).

27. T. Tsuda et al., *ECS Trans.*, **50**, 239–250 (2013).

28. S. Higashino et al., *J. Electroanal. Chem.*, **912**, 116238 (2022).

29. I. -Wen Sun, A. G. Edwards, and G. Mamantov, *J. Electrochem. Soc.*, **140**, 2733–2739 (1993).

30. T. Nohira, T. Ide, X. Meng, Y. Norikawa, and K. Yasuda, *J. Electrochem. Soc.*, **168**, 46505 (2021).

31. D. F. Roeper, K. I. Pandya, G. T. Cheek, and W. E. O'Grady, *J. Electrochem. Soc.*, **158**, F21–F28 (2011).

32. Z. Ke et al., *Ceram. Int.*, **46**, 12767–12772 (2020).

33. E. Gunnell et al., *J. Electrochem. Soc.*, **168**, 046501 (2021).

Supplementary Materials

Toward Tungsten Electrodeposition at Moderate Temperatures Below 100 °C Using Chloroaluminate Ionic Liquids

Shota Higashino,[1,2,*] Yoshikazu Takeuchi,[2] Masao Miyake,[2] Takuma Sakai[1], Takumi Ikenoue,[2] Masakazu Tane,[1] and Tetsuji Hirato[2]

[1]Graduate School of Engineering, Osaka Metropolitan University, Sugimoto, Sumiyoshi-ku, Osaka 558-8585, Japan

[2]Graduate School of Energy Science, Kyoto University, Yoshida-honmachi, Sakyo-ku, Kyoto 606-8501, Japan

*Corresponding Author: higashino@omu.ac.jp

Results and discussion

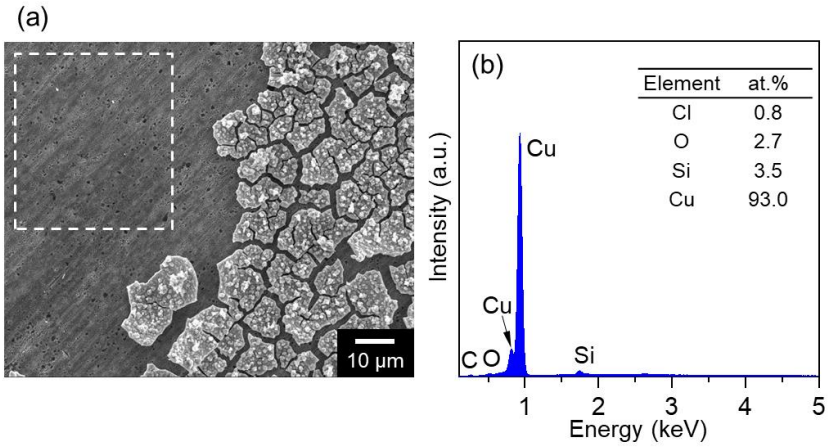

Supplementary Figure S1. (a) SEM image of the Cu electrode surface after potentiostatic electrolysis in the EMIC–$AlCl_3$–WCl_5 bath at +0.1 V and 80 °C. (b) EDX spectrum for the dotted area in (a), where the deposits were completely exfoliated.

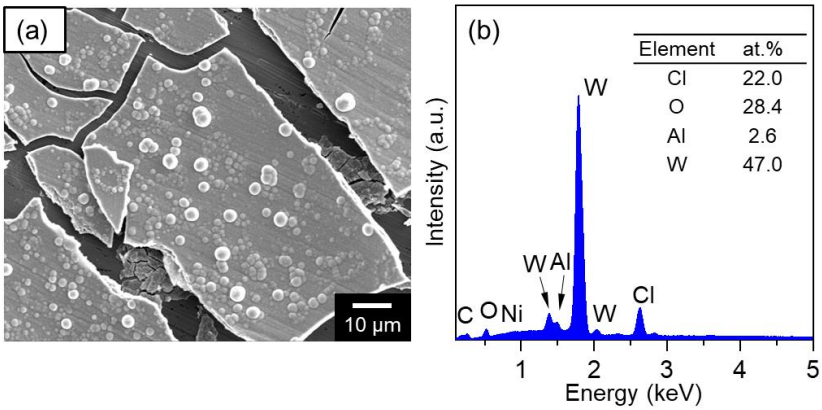

Supplementary Figure S2. (a) SEM image and (b) EDX spectrum of the Ni electrode surface after potentiostatic electrolysis in the EMIC–$AlCl_3$–WCl_5–KF bath at +0.1 V and 80 °C.